Thai Journal of **Math**ematics
Volume 21 Number 4 (2023)
Pages 979–990

http://thaijmath.in.cmu.ac.th

ISSN 1686-0209

Discrete and Computational Geometry, Graphs, and Games

Parallel Curve Detection Method based on Hough Transform

Nattapol Chanpaisit and Pat Vatiwutipong*

Kamnoetvidya Science Academy, Rayong, Thailand
e-mail: pat.v@kvis.ac.th (P. Vatiwutipong)

Abstract Hough transform is a widely used approach for recognizing straight lines and circles. Recently, an extension was published, allowing us to detect a larger class of algebraic curves. The image with parallel curves is the subject of this study. An incorrect curve may be detected using the standard approach. We modify the accumulator function and introduce the concept of parallel curves into the detection method to tackle this problem. Synthetic and real-world images are used to demonstrate the effectiveness of this method.

MSC: 14Q05; 68U10; 14H50
Keywords: parallel curves; algebraic plane curves; pattern recognition; Hough transform

Submission date: 07.01.2022 / Acceptance date: 05.05.2023

1. Introduction

The Hough transform was a technique used to detect curves in an image, which P.V.C. Hough introduced in 1962, as seen in [1]. The early usages of this technique were only to detect straight lines and circles from digital images, as in [2]. The method uses a voting procedure where points in the image space are converted to the parameter space or Hough space. This creates a set of possible parameters that are contained in a function called the accumulator function. The corresponding lines were transformed from points lying on the same curve in image space intersecting at the same point in Hough space. After all possible iterations to transform all points, Hough space peaks at the parameter of the corresponding curve that contain the most points in image space. A formal definition of Hough Transform and its properties was provided in [3]. An extension of the Hough transform to a more general algebraic curve was introduced by M.C. Beltrametti in [4] and [5]. This allowed us to detect any irreducible plane curve which satisfied the Hough regularity property using Hough Transform.

In this study, we focus on images consisting of parallel curves. If any points from different curves are accidentally joined, the detection may fail because the accumulator

*Corresponding author.

Published by The Mathematical Association of Thailand.

function will reach a peak at a more prominent curve that was not parallel to the others. Take the image of a banana leaf as shown in Figure 1 as an example. If we aim to extract the direction of parallel veins, the Hough transform will mislead us to the midrib because there were more points on that line than on each parallel vein. To avoid this kind of detection of the unintended non-parallel curve, we add a parallel assumption to our modified approach.

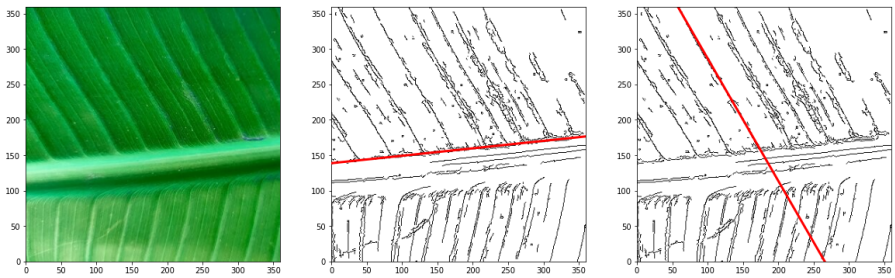

FIGURE 1. The input image of the real leaf (a); line detected directly from Hough transform plotted in the edge map (b); the example of desired parallel line plotted in the edge map (c).

This issue also occurs when the image of circles of different sizes with the same center, which are parallel, such as annual rings of wood or a cross-section of an onion image. The definition of parallel is extended from lines to any algebraic curves. Detecting the parallel irreducible algebraic curve relies on the Hough Transform and the modification of the accumulator function. We also introduce specific terms and definitions for the property of a curve that enabled the curve to be detected with our proposed method. The methodology's performance is compared to the usual method by using synthetic images containing a variety of shapes.

2. PRELIMINARIES

Before introducing the definition of parallel, we begin with the notation of a curve and a family of curves.

Definition 2.1. For $t \in \mathbb{N}$ tuples of independent parameters $\lambda := (\lambda_1, \ldots, \lambda_t) \in \mathbb{R}^t$, let $f_\lambda : \mathbb{R}^n \to \mathbb{R}$ be a function parametrized by λ. Define a curve correspond with f_λ by $C_\lambda = \{(x_1, \ldots, x_n) : f_\lambda(x_1, \ldots, x_n) = 0\}$ and a family of curves $\mathcal{F} = \{C_\lambda : \lambda \in \mathbb{R}^t\}$.

For the algebraic plane curves in xy-Cartesian coordinates that this study focused on, the indeterminates are x and y.

Generally, parallel curves are curves that do not intersect one another. However, we extend the definition of the term parallel, which is redefined as $\mathcal{L}-$parallel, to describe the parameter that varied between the two curves while all remaining parameters that were not parallel had to share the same value. The case of the parallel straight lines is one example of $\mathcal{L}-$parallel on the distance from the origin of the straight lines. The definition of $\mathcal{L}-$parallel of the curve on any parameter is as follows.

Definition 2.2. Consider a set $\mathcal{L} \subset \{1, \ldots, t\}$. A curve C_λ is said to by $\mathcal{L}-$parallel to a curve $C_{\lambda'}$ if $\lambda_i = \lambda'_i$ for all $i \notin \mathcal{L}$. Moreover, we call the parameters corresponding to the index in the set $\mathcal{L}$ as parallel parameters.

Example 2.3. Let $C_\lambda : r_1 - x\cos\theta_1 - y\sin\theta_1 = 0$ and $C_{\lambda'} : r_2 - x\cos\theta_2 - y\sin\theta_2 = 0$ be two straight lines, where $\lambda = (r, \theta)$ is a parameter. They are $\mathcal{L}-$parallel for $\mathcal{L} = \{1\}$ if $\theta_1 = \theta_2$, that is their angles to the x-axis are equal, see Figure 2(a). This is equivalent to the usual parallel definition. In contrary, if $r_1 = r_2$, then we say that it is $\mathcal{L}-$parallel for $\mathcal{L} = \{2\}$ instead, see Figure 2(b). Notice that, in this case, these parallel lines may be intersected.

Example 2.4. Let $C_\lambda : (x-h_1)^2+(y-k_1)^2-r_1^2 = 0$ and $C_{\lambda'} : (x-h_2)^2+(y-k_2)^2-r_2^2 = 0$ be two circles, where λ denote the parameter vector (h, k, r). They are $\mathcal{L}-$parallel for $\mathcal{L} = \{3\}$ if $h_1 = h_2$ and $k_1 = k_2$, that is, their share the same center, see Figure 3(a). In contrary, if $r_1 = r_2$, then we say that it is $\mathcal{L} = \{1, 2\}$ instead, see Figure 3(b).

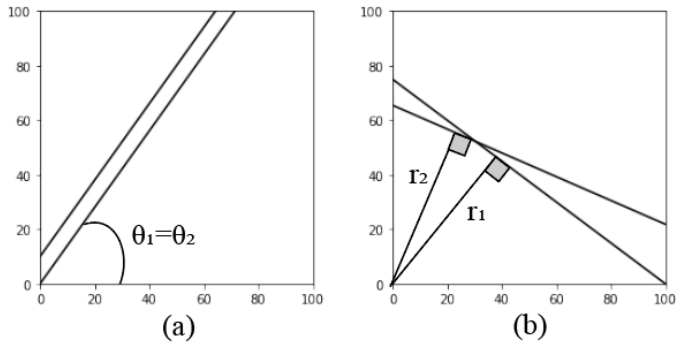

FIGURE 2. (a) $\mathcal{L}$-parallel lines for $\mathcal{L} = \{1\}$; (b) $\mathcal{L}$-parallel lines for $\mathcal{L} = \{2\}$

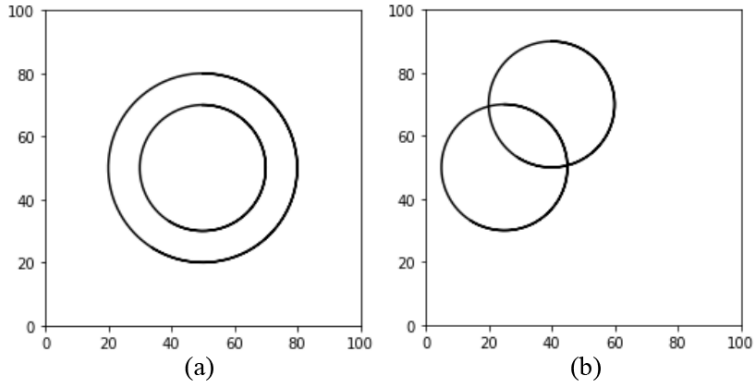

FIGURE 3. (a) $\mathcal{L}$-parallel circles for $\mathcal{L} = \{1\}$; (b) $\mathcal{L}$-parallel circles for $\mathcal{L} = \{2, 3\}$

Let $\mathcal{F}$ be a family of curves parametrized by $\lambda \in \mathbb{R}^t$. For $\mathcal{L} \subset \{1, \ldots, t\}$ and fix $\lambda^{(0)} \in \mathbb{R}^t$. We denoted a subfamily of all curves in $\mathcal{F}$ that are $\mathcal{L}-$parallel to a curve $C_{\lambda^{(0)}}$ by $\mathcal{F}_{\mathcal{L},\lambda^{(0)}}$. To determine important properties of a family of curves that allow us to detect parallel curves based on the Hough transform, we defined two other terms: cover and partition.

Definition 2.5. Let $\mathcal{F}_{\mathcal{L},\lambda^{(0)}}$ be a family of curves.

(1) We say that it is a cover if: $\bigcup_{\mathcal{C}_\lambda \in \mathcal{F}_{\mathcal{L},\lambda^{(0)}}} \mathcal{C}_\lambda = \mathbb{R}^n$. This definition simply means that for any point in $\mathbb{R}^n$, there must be a curve in the family passing through.

(2) We say that it is a partition if: $\mathcal{F}_{\mathcal{L},\lambda^{(0)}}$ is a cover and for all distinct $\mathcal{C}_\lambda, \mathcal{C}_{\lambda'} \in \mathcal{F}_{\mathcal{L},\lambda^{(0)}}$, we have $\mathcal{C}_\lambda \cap \mathcal{C}_{\lambda'} = \varnothing$ or $\mathcal{C}_\lambda = \mathcal{C}_{\lambda'}$. This is equivalent to the subfamily being a partition if it is a cover and all curves do not intersect which one another.

Back to the subfamily of curves in Example 2.3 and 2.4, the following example demonstrated the properties of curves for each combination of set $\mathcal{L}$.

Example 2.6. For $\mathcal{L} = \{1\}$, a subfamily $\mathcal{F}_{\mathcal{L},(r,\theta_0)}$ is the set of all straight lines such that the angle between it and the x-axis is equal to θ_0. This subfamily is a partition; see Figure 4(a). For $\mathcal{L} = \{2\}$, a subfamily $\mathcal{F}_{\mathcal{L},(r_0,\theta)}$ is the set of all straight lines such that the distance between it and the origin is equal to r_0. This subfamily is not a cover as all curves cannot pass through the point where the distance from the origin is less than r_0; see Figure 4(b). Consequently, this subfamily is not a partition.

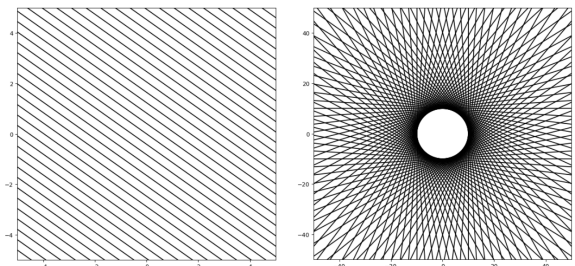

FIGURE 4. (a) Illustration of curves in the subfamily $\mathcal{F}_{\mathcal{L},(r,\theta)}$ as $\mathcal{L} = \{1\}$; (b) illustration of curves in the subfamily $\mathcal{F}_{\mathcal{L},(r,\theta)}$ as $\mathcal{L} = \{2\}$

Example 2.7. For $\mathcal{L} = \{3\}$, a subfamily $\mathcal{F}_{\mathcal{L},(h_0,k_0,r)}$ is the set of all circles with the same center at (h_0, k_0). This subfamily is a cover and a partition; see Figure 5(a). For $\mathcal{L} = \{1, 2\}$, a subfamily $\mathcal{F}_{\mathcal{L},(h,k,r_0)}$ is the set of all circles with fixed radius r_0. This subfamily is a cover but not a partition; see Figure 5(b).

Next, we will state the definition of Hough transform, which is followed from [5–7].

Definition 2.8. For a family $\mathcal{F}$ of curve defined by $f_{\lambda_1,\ldots,\lambda_t}(x_1, \ldots, x_n)$ and $P = (x_{P_1}, \ldots, x_{P_n})$ be a point in $\mathbb{R}^n$. Let $\Gamma_P(\mathcal{F})$ be the hyper-surface defined on a space $\mathbb{R}^t$ by

$$f_{\Lambda_1,\ldots,\Lambda_t}(x_{P_1}, \ldots, x_{P_n}),$$

where $\Lambda_1, \ldots, \Lambda_t$ is the tuple of indeterminate. We say that $\Gamma_P(\mathcal{F})$ is the Hough transform of point P with respect to family $\mathcal{F}$ and $\mathcal{H}_\mathcal{F}$ is the accumulator function.

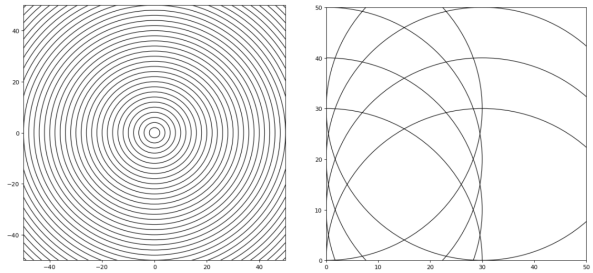

FIGURE 5. (a) Illustration of curves in the family $\mathcal{F}_{\mathcal{L},(h_0,k_0,r)}$ as $\mathcal{L} = \{3\}$; (b) illustration of curves in the family $\mathcal{F}_{\mathcal{L},(h,k,r_0)}$ as $\mathcal{L} = \{1, 2\}$

As the indeterminate change from $(\lambda_1, \ldots, \lambda_t)$ to $(\Lambda_1, \ldots, \Lambda_t)$, the accumulator function collected the value at the possible set of parameters of the curve passing through a given point in the image space, and for points in the same curve in image space, the corresponding curve in Hough space will intersect at exactly one point, see [6]. Moreover, the distinct curves in the image space give different intersections of the curve in Hough space, but the intersection will be at the exact value of the parallel parameter.

3. Parallelism Detection Algorithm for Curves

We utilize properties of curves that can be defined by an irreducible polynomial as in the definition 3.1.

Definition 3.1. For $t \in \mathbb{N}$ tuples of independent parameters $\lambda := (\lambda_1, \ldots, \lambda_t) \in \mathbb{R}^t$ and some constant degrees $d \in \mathbb{N}$, let

$$f_\lambda(x_1, \ldots, x_n) = \sum_{k_1+\cdots+k_n \le d} x_1^{k_1} \cdots x_n^{k_n} g_{k_1,\ldots,k_n}(\lambda_1, \ldots, \lambda_t) \tag{3.1}$$

be a family of irreducible polynomials characterized by the indeterminate $x_1, \ldots, x_n$. We will call the curve $\mathcal{C}_\lambda = \{(x_1, \ldots, x_n) : f_\lambda(x_1, \ldots, x_n) = 0\}$ as irreducible curve when $f_\lambda(x_1, \ldots, x_n)$ is a irreducible polynomial.

After observing the value of the accumulator function on irreducible curves, we found that if there are parallel curves in the image, then the accumulator function in that direction will contain peaks at each position of the curves. On the other hand, there is only one very high rise in the accidentally lined-up direction. The following theorem is the conceptual idea for our proposed parallel curve recognition method.

Theorem 3.2. *Let $\mathcal{F}$ be a family of irreducible curves parametrized by t dimensional tuple. For $\mathcal{L} \subset \{1, \ldots, t\}$, then the following hold.*

(1) Fix $\lambda^{(0)}$. For each λ such that $C_\lambda \in \mathcal{F}_{\mathcal{L},\lambda^{(0)}}$, the Hough transform $\Gamma_P(\lambda)$ of the pairs (C_λ, P) when P varies on C_λ all pass through a point on set $E_{\mathcal{L},\lambda^{(0)}} = \{\Lambda \in \mathbb{R}^t : \Lambda_i = \lambda_i^{(0)}$ for all $i \notin \mathcal{L}\}$.

(2) Fix $\lambda^{(0)}$. If the Hough transform $\Gamma_P(\lambda)$ of the pairs (C_λ, P) when P varies on curves C_λ and the Hough transform $\Gamma_{P'}(\lambda)$ of the pairs $(C_{\lambda'}, P')$ when P' varies

on curves $C_{\lambda'}$ in $\mathcal{F}$ are all intersected at two points in the set $E_{\mathcal{L},\lambda^{(0)}}$, then C_λ is $\mathcal{L}-$parallel to $C_{\lambda'}$.

Proof. Without loss of generality, suppose that $\mathcal{L} = \{1,\dots,\ell\}$. Let $\lambda \in \mathbb{R}^t$ such that $\mathcal{C}_\lambda \in \mathcal{F}_{\mathcal{L},\lambda^{(0)}}$. So, for each f_λ, define

$$f_{\mathcal{L},\lambda}(x_1,\dots,x_n) = \sum_{k_1+\cdots+k_n\le d} x_1^{k_1}\cdots x_n^{k_n} g_{k_1,\dots,k_n}(\lambda_1,\dots,\lambda_\ell,\lambda^{(0)}_{\ell+1},\dots,\lambda^{(0)}_n). \quad (3.2)$$

parametrized by only ℓ parameters. Then, its Hough transform $\Gamma_P(\lambda_1,\dots,\lambda_\ell)$ is defined by

$$\sum_{k_1+\cdots+k_n\le d} x_{P_1}^{k_1}\cdots x_{P_n}^{k_n} g_{k_1,\dots,k_n}(\Lambda_1,\dots,\Lambda_\ell,\lambda^{(0)}_{\ell+1},\dots,\lambda^{(0)}_n) = 0, \quad (3.3)$$

in the ℓ indeterminate $\Lambda_1,\dots,\Lambda_\ell$. By Theorem 2.2.1 of [5], $\Gamma_P(\lambda_1,\dots,\lambda_\ell)$ all pass through the point $(\lambda_1,\dots,\lambda_\ell)$. This leads to our first result. To prove the second statement, the fact that $\Gamma_P(\lambda)$ are all intersect the set $\{\Lambda \in \mathbb{R}^t : \Lambda_i = \lambda_i^{(1)} \text{ for all } i \notin \mathcal{L}\}$ implies that $\Gamma_P(\lambda)$ pass through some point $(\lambda'_1,\dots,\lambda'_\ell,\lambda^{(1)}_\ell,\dots,\lambda^{(1)}_n)$. By Theorem 2.2.2 of [5], we have $\mathcal{C}_{\lambda_1,\dots,\lambda_\ell,\lambda^{(0)}_{\ell+1},\dots,\lambda^{(0)}_t} = \mathcal{C}_{\lambda'_1,\dots,\lambda'_\ell,\lambda^{(1)}_{\ell+1},\dots,\lambda^{(1)}_t}$. Hence, the result is obtained. ∎

The prior procedure of preventing this false detection is to integrate over all directions in $\mathcal{L}$, that is

$$\int_{\mathbb{R}}\cdots\int_{\mathbb{R}} \mathcal{H}_\mathcal{F}|_{E_{\mathcal{L},\lambda^{(0)}}}(\Lambda)d\Lambda_1\dots d\Lambda_\ell \quad (3.4)$$

where $\mathcal{H}_\mathcal{F}$ is an accumulator function. However, we can show that the integration (as a function of parallel parameter or array with parallel parameters as its axis) will be constant for a partition subfamily $\mathcal{F}_{\mathcal{L},\lambda^{(0)}}$.

Lemma 3.3. *If the subfamily $\mathcal{F}_{\mathcal{L},\lambda^{(0)}}$ is a partition, $\int_{\mathbb{R}}\cdots\int_{\mathbb{R}} \mathcal{H}_\mathcal{F}|_{E_{\mathcal{L},\lambda^{(0)}}}(\Lambda)d\Lambda_1\dots d\Lambda_\ell$ is a constant function.*

Proof. Since $\mathcal{F}_{\mathcal{L},\lambda^{(0)}}$ is a partition, for each $P \in \mathbb{R}^n$ there is exactly one $\mathcal{C}_\lambda \in \mathcal{F}_{\mathcal{L},\lambda^{(0)}}$ such that $P \in \mathcal{C}_\lambda$. Then $\Gamma_P[\mathcal{F}]$ is intersected with $E_{\mathcal{L},\lambda^{(0)}} = \{\Lambda \in \mathbb{R}^t : \Lambda_i = \lambda_i^{(0)} \text{ for all } i \notin \mathcal{L}\}$ at exactly one point. Since

$$\mathcal{H}_\mathcal{F}[P]|_{E_{\mathcal{L},\lambda^{(0)}}}(\Lambda) = \begin{cases} m(P) & ;\Lambda \in \Gamma_P(\mathcal{H}) \cap E_{\mathcal{L},\lambda^{(0)}} \\ 0 & ;\text{otherwises} \end{cases} \quad (3.5)$$

we have

$$\mathcal{H}_\mathcal{F}[m]|_{E_{\mathcal{L},\lambda^{(0)}}}(\Lambda) = \sum_{P\in\mathcal{C}_\lambda\in\mathcal{F}_{\mathcal{L},\lambda^{(0)}}} m(P). \quad (3.6)$$

We integrate both sides of the equation (3.6) over the image space. The right-hand side of the equation will become the integration of the whole image m, which is a constant. This leads to the result. ∎

As a result, we shall first apply some function F to the integrand rather than integrating directly. The function should be convex and increasing. Otherwise, the order of the accumulator function will be lost. We recommend using a simple function such as the

square function, soft thresholding, or hard thresholding function. Our proposed method is, instead of seeking the maximum of the accumulator function, we seek the peak of

$$\int_{\mathbb{R}} \cdots \int_{\mathbb{R}} F\big(\mathcal{H}_{\mathcal{F}}|_{E_{\mathcal{L},\lambda^{(0)}}}(\Lambda)\big) d\Lambda_1 \ldots d\Lambda_\ell \tag{3.7}$$

where F was an accumulator function. That provides us with the direction of the parallel curves. After that, we project the accumulator function on $\mathbb{R}^\ell$ and consider its peaks to obtain the positions on those parallel curves.

We utilize the property of the convex function. Let φ be a convex function, then for any number real number $x_1, x_2, \ldots, x_n$ the following inequality hold.

$$n\varphi\left(\frac{\sum x_i}{n}\right) \leq \sum \varphi(x_i). \tag{3.8}$$

Consider the integral of the accumulator function over parallel parameters (the integral as a function of non-parallel parameters) so that the corresponding parallel curves do not exist in the image. The value of the accumulator function along this parallel parameter is random and distributed almost equally. The integral of the accumulator function along these parallel parameters is a lower bound of the inequality 3.8. Consequently, when we apply a convex increasing function φ to an accumulator function, the integration $\int_{\mathbb{R}} \cdots \int_{\mathbb{R}} \varphi\big(\mathcal{H}_{\mathcal{F}}|_{E_{\mathcal{L},\lambda^{(0)}}}(\Lambda)\big) d\Lambda_1 \ldots d\Lambda_\ell$ reach a peak at a certain non-parallel parameter corresponding to the prominent parallel curves in the image.

The flow for our proposed algorithm for detecting the parallelism of curves is as follows:

Step 1. Converting the image into an edge map using edge Detection algorithm (e.g., Canny edge detector [8] and Laplacian of Gaussian (LoG)).

Step 2. Applying Hough transform to the edge map. After we get an edge map, the accumulator function can be derived as a sum of the Hough transform. The process of Hough transform can be referred to [5].

Step 3. Applying some convex function to the accumulator function.

Step 4. Identifying the non-parallel parameter that produces the maximum value of the integral of the accumulator function.

Step 5. Applying the peak finding algorithm to the accumulator function along with the maximum non-parallel parameter in step 4 to find parallel parameters of multiple parallel curves in the image.

4. Experimental Results and Discussion

This section presents several examples involving both synthetic and real-world images. For the first example, we consider the perceptually parallel straight-line binary image as shown in Figure 6(a).

The irreducible polynomial form for straight lines can be parametrized by $\lambda = (m, c)$ where m is the slope of the straight line, and c is the $Y-$intercept of the line. The curve can be expressed as $C_\lambda : y - mx - c = 0$. However, since the slope cannot be bounded by constant, straight lines are usually parametrized by $C_\lambda : r - x\cos\theta - y\sin\theta = 0$ instead, where (r, θ) is the parameter. The properties in 3.2 still hold for this parameterization; see [9].

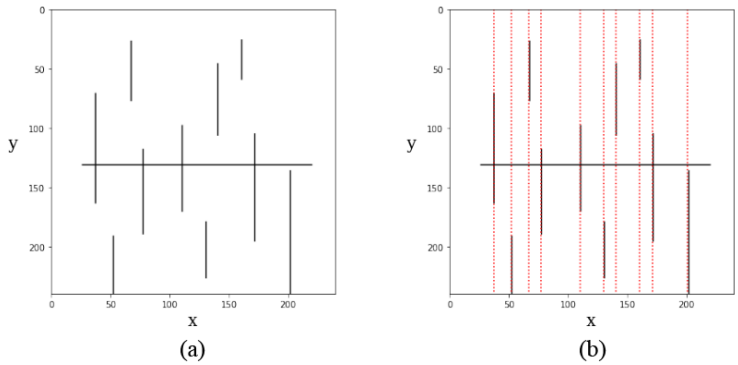

FIGURE 6. (a) The synthetic input image; (b) detected parallel lines

In Figure 6(a), we intend to detect the parallel straight lines that lie vertically, and in this example, our proposed method shows the results as intended, the red dash lines in Figure 6(b). We parameterize the straight lines with $r = x\ cos\theta + y\ sin\theta$, where (x, y) is our coordinate in real vector space $\mathbb{R}^2$, and (r, θ) is our parameter. After we apply the Hough transform to the image to get a 2-dimensional accumulator function (as a function of r and θ), see Figure 7(a).

The integral without applying a convex function in Figure 7(b) turns out to be constant. This agrees with the theorem 3.3. In Figure 7(c), we use the square function as our convex function. The integral as a function of θ (our non-parallel parameter) peaks at $\theta = 90$ degrees. When we plot the accumulator function along with $\theta = 90$ degrees, we obtained different peaks corresponding to the distance from origin r of different parallel curves in the image (see Figure 7(d)). Then, we plot these curves back in Figure 6(b).

We notice that the horizontal distraction line is the longest line in the image, so the corresponding value in the accumulator function is greater than the shorter vertical lines. We notice in Figure 7(c) that the peak at $\theta = 0$ degrees is only slightly less than the peak at $\theta = 90$ degrees, and if this distraction line is more prominent than the parallel line, our detection method may fail.

Next, we apply the proposed method to the synthetic image containing parallel circles as shown in Figure 8(a). We parameterize the circle as $C_\lambda : (x-h)^2 + (y-k)^2 - r^2 = 0$. Then the accumulator function is a discrete multivariate function of (h, k, r). Since we wish to detect the parallel circles that share the same center, this is a case for $\mathcal{L}-$parallel for $\mathcal{L} = 3$, varying radius r. After we get the accumulator function, we integrate it along the radius r (parallel parameter) to get the integral as a function of (h, k). Then the maximum in the integral, as illustrated by the blackest point in the integral heat map in Figure 9(b), is at the center, non-parallel parameters, of the parallel circle. We consider the accumulator function again to find peaks along with this maximum center point. The peaks correspond to a different parallel parameter of different curves, see Figure 9(c), and we plot the detected curves back into the input image, see Figure 8(b).

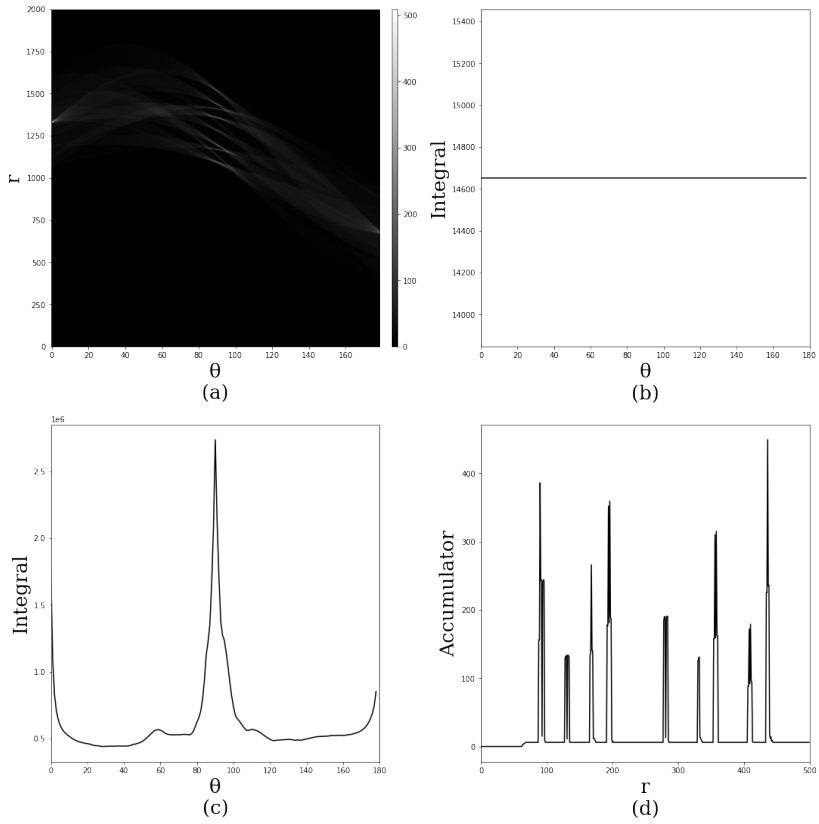

FIGURE 7. (a) Accumulator function heat map; (b) integral of accumulator function; (c) integral of accumulator function after applying the square function; (d) accumulator function along the detected non-parallel parameter

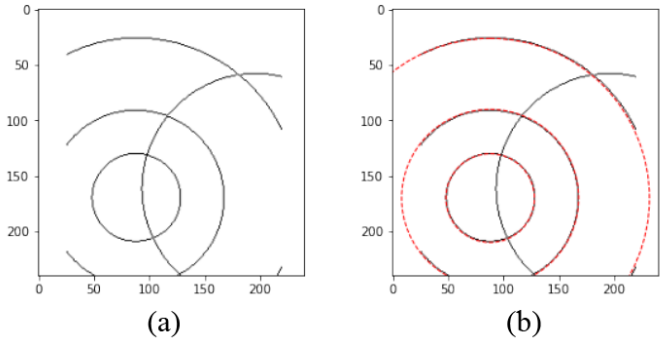

FIGURE 8. (a) Synthetic Input image; (b) Detected parallel circles

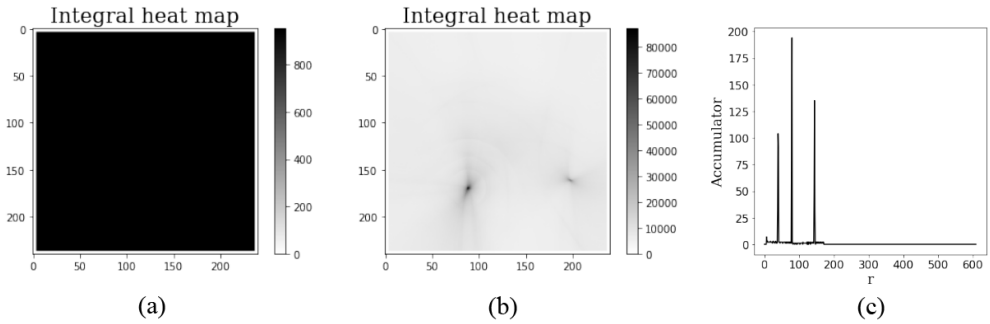

FIGURE 9. (a) Integral heat map without applying any convex function; (b) integral heat map after applying the square function; (c) accumulator function along the detected non-parallel parameter

In the following example, we demonstrate the detection of parallel veins of the plant leaf, where the noises are more prominent than in previous synthetic image examples; see Figure 10(a).

In this section, an application of their method to a colored close-up image of a leaf is described. The image is first converted into an edge map using the Canny edge detector. Then the Hough transform is applied to calculate the accumulator function as a function of (r, θ) from all the salient points in the edge map. The integral of the accumulator function as a function of θ is plotted in Figure 11(b), and the integral of the squared accumulator function is plotted in Figure 11(c). The detected lines are at $\theta = 60$ degrees, and the accumulator function is along $\theta = 60$ degrees is illustrated in Figure 11(d). Note that their method could detect not only the midrib of the leaf but also the parallel veins in the lower part of the leaf at $\theta = 102$ degrees. However, the parallel lines for the midrib are more sensitive to their detection method than the parallel veins because the midribs were significantly longer.

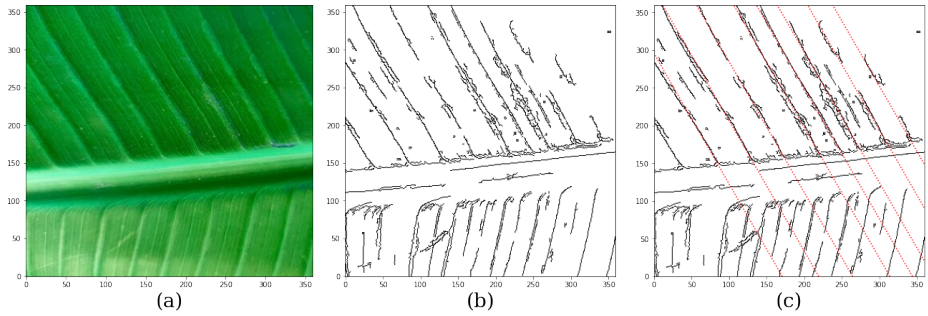

FIGURE 10. (a) Input image; (b) edge map; (c) detected lines

As the Hough transform process varies for different types of curves, our computational complexity varies from curve to curve. The complexity of our proposed algorithm could be separated into three parts: edge detection, Hough transform, and integration. The

resolution of our input image is $n \times n$. Edge detection involves the convolution filter going through each block of pixels for a total of n^2 times, so the fastest time complexity for the edge detection algorithm is in $\mathcal{O}(n^2)$, regardless of the type of curves. Next, the discretized unit of parameters was all equal to m, the number of salient points in the edge map was N, and the number of parameters was t. For the Hough transform, we need to iterate over all the salient points in the image. Then, for each point, we need to couple it with each pixel for $t-1$ parameters. Taking all these processes into consideration, the complexity for the Hough transform is $\mathcal{O}(Nn^2m^{t-1})$. The complexity of integration is $\mathcal{O}(m^t)$ since we needed to iterate over all combinations of parameters in the accumulator function. Accordingly, the complexity of our method is $\mathcal{O}(Nn^2m^{t-1} + Nm^t)$.

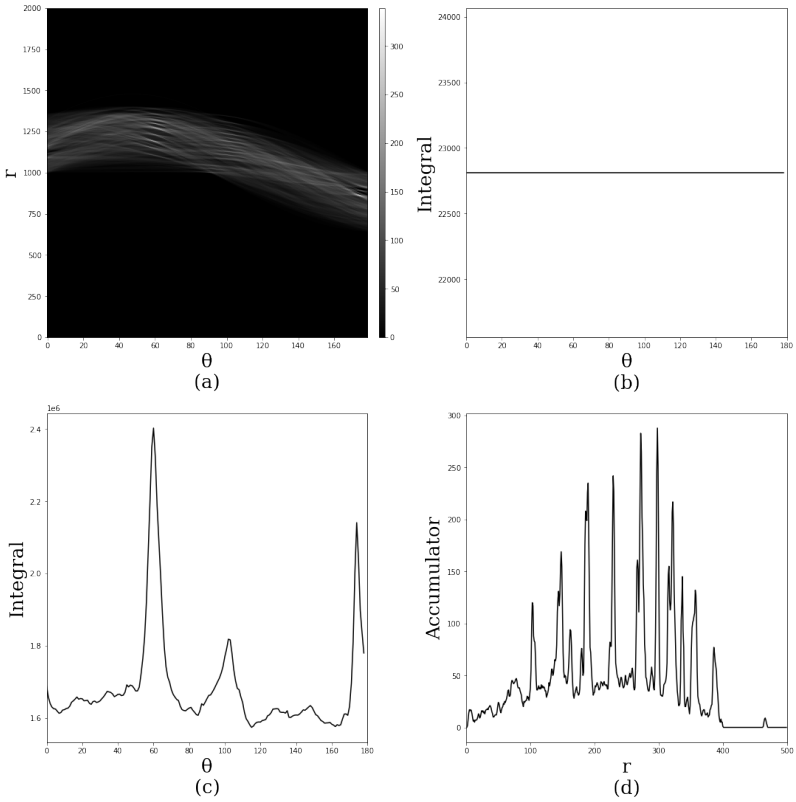

FIGURE 11. (a) Accumulator function heat map; (b) integral plot without applying any convex function; (c) integral plot after applying square function; (d) accumulator plot along detected non-parallel parameter

REFERENCES

[1] P.V.C. Hough, Method and means for recognizing complex patterns, U.S. Patent (1962) US 3069654.

[2] R.O. Duda, P.E. Hart, Use of the Hough transformation to detect lines and curves in pictures, Comm. ACM 15 (1972) 11–15.

[3] J. Princen, J. Illingworth, J. Kittler, A formal definition of the Hough transform: Properties and relationships, Journal of Mathematical Imaging and Vision 1 (2) (1992) 153–168.

[4] C.M. Beltrametti, L. Robbiano, An algebraic approach to Hough transforms, Journal of Algebra 371 (2012) 669–681.

[5] M.C. Beltrametti, A.M. Massone, M. Piana, Hough transform of special classes of curves, SIAM J. Imaging Sci. 6 (1) (2013) 391–412.

[6] G. Ricca, M.C. Beltrametti, A.M. Massone, Detecting curves of symmetry in images via Hough transform, Math. Comput. Sci. 10 (2016) 179–205.

[7] M.C. Beltrametti, C. Campi, A.M. Massone, M. Torrente, Geometry of the Hough transforms with applications to synthetic data, Math. Comput. Sci. (2020).

[8] J. Canny, A computational approach to edge detection, in IEEE Transactions on Pattern Analysis and Machine Intelligence 8 (6) (1986) 679–698.

[9] R.O. Duda, P.E. Hart, Use of the Hough transformation to detect lines and curves in pictures, Commun. ACM 15 (1) (1972) 11–15.